Resonant Converter Based Contactless Power Supply for Robots and Manipulators

Received 5th December 2007; accepted 18th January 2008.

Artur Moradewicz, Marian P. Kaźmierkowski

Abstract:

This paper presents an inductive Contactless Power Supply (CPS) system for robots and manipulators. The energy is transmitted using rotatable transformer with adjustable air gap and power converter. To minimize total losses of the system a series resonant circuit is used. It ensures zero current switching (ZCS) condition for MOSFET power transistors. The controller and protection are implemented in FPGA system. The resonant frequency is adjusted by extreme regulator, which follows instantaneous value of primary peak current. Some simulated and experimental results, which illustrate operation of developed 3 kW laboratory model, are presented.

Keywords: *energy transmission, contactless power supply, series resonance converter, FPGA control.*

1. Introduction

The contactless power supply (CPS) systems are recently developed and investigated widely [3, 5-9]. This innovative technology creates new possibilities to supply mobile devices with electrical energy because elimination of cables and/or slip rings increases reliability and maintenance-free operation of such critical systems as in aerospace, biomedical and robotics applications. The core of CPS system is inductive or capacitive coupling and high switching frequency converter. The capacitive coupling is used in low power range (sensor supply systems) whereas inductive coupling allows power transfer from a few mW up to hundred kW [5]. The basic structure of the inductive coupled power supply system for robots is shown in Fig. 1. The indirect DC link AC/DC/AC power converter generates a square wave voltage of 200 V and 60 kHz. This voltage is fed to the primary winding of first rotatable transformer located on the first axis of the robot. The transformer secondary side is connected to the next DC link AC/DC/AC power converter, which uses pulse width modulation (PWM) technique, generates variable frequency AC voltage to supply first three-phase machine. The transformer secondary is also connected to the primary of the next rotatable transformer, which is located on the second joint of the robot. The transformer feeds the second axis drive in similar way as described above for the first machine. More transformers may be added to create arrangement of an AC bus throughout the robot.

This paper reports on a newly developed inductive CPS system with a rotatable transformer and MOSFET based resonant converter. The novelty of the system lies in application of high switching frequency MOSFET resonant converter and FPGA implementation of extreme regulator for control and protection circuit. Simulation and experimental results of 3 kW prototype system are presented.

2. Configuration of inductive contactless energy transmission (CET) system

In further presentation only inductive energy transmission (CET) part (without PWM inverter-fed drives) of the whole CPS system of Fig. 1 will be discussed. The configuration of the experimental inductive CET system

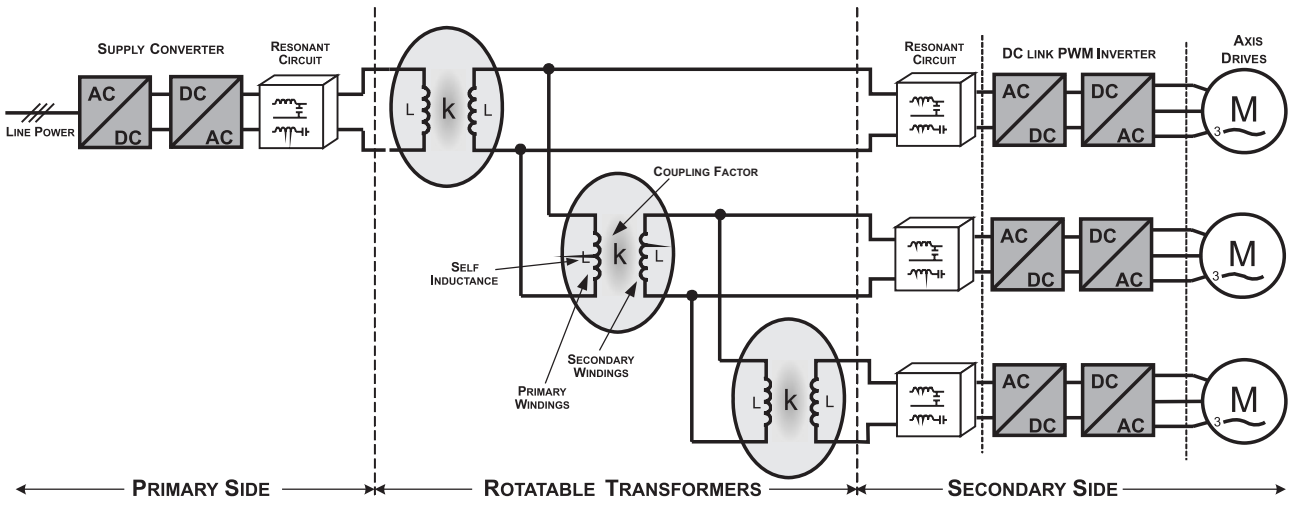

Fig. 1. Basic structure of contactless power supply (CPS) for multiaxis robots.

is shown in Fig. 2. The core of the system is a rotatable transformer with an air gap, which (in our experimental set-up) can be adjusted up to 2.8 cm large. At the energy feeding input end is a full bridge MOSFET inverter and at the secondary side an electronic consumer module (where Ro represents PWM inverter and motor) with bridge diode rectifier is connected. This solution has following advantages: secondary circuits can be rotatable relative to primary, control and power supply system is located on the primary side and is electrically and mechanically separated from the secondary circuit.

In conventional applications transformer is use for galvanic insulation between source and load, and its operation is based on high magnetic coupling coefficient k between primary and secondary windings. Because of used two halves cores and air gap, CET transformers operate under much lower magnetic coupling factor k. As a result the main inductance L_{12} is very small whereas leakage inductances (L_{11}, L_{22}) are large as compare with conventional transformers. Consequently, the magnetizing current increase causes higher conducting losses. Also, winding losses increase because of large leakage inductances. Another disadvantage of transformers with relatively large gap is EMC problem (strong radiation). To minimize above mentioned disadvantages of CET transformers several power conversion topologies have been proposed, which can be classified in following categories: the fly back, resonant, quasi-resonant and self-resonant [1, 2]. The common for all these topologies is that they all utilize the energy stored in the transformer. In this work resonant soft switching technique has been used. To form resonant circuits two methods of leakage inductances compensation can be applied: S-series or P-parallel giving four basic topologies: SS, SP, PS, and PP (first letter denotes a primary and second a secondary compensation). PS and PP require an additional series inductor to regulate the inverter current flowing into the parallel resonant tank.

This additional inductor increase EMC distortion and total cost of CET system. Therefore, only SS and SP topology has been considered.

If we assume the same numbers of primary and secondary winding $n_1 = n_2$, the inductances of presented transformer can be described by following equations:

$$\begin{aligned} L_1 &= L_{11} + L_{12} & L_1 &= L_{11} + L_{12} \\ L_2 &= L_{22} + n^2 L_{12} \Rightarrow & L_2 &= L_{22} + L_{12} \\ M &= nL_{12} & M &= L_{12} \end{aligned} \tag{1}$$

where:

(2)

$$L_1 = L_2 = L,\ L_{11} = L_{22} = L - M = \frac{1-k}{k} M,\ k = M / L$$

If the fundamental component of $u_2(t)$ is in phase with $i_2(t)$, the output rectifier with capacitive filter behaves as load resistance transformer. The value of this equivalent resistance is equal to [1]:

$$R_e = \frac{8}{\pi^2} R_o = 0.8106 \cdot R_o \tag{3}$$

Impedance of secondary side, depending on chosen compensation topology, is:

- for series compensation:

$$Z_C = R_e + jX_2 \tag{4}$$

- for parallel compensation:

$$Z_C = \left\{ j\omega L_{11} + 1/(j\omega \cdot C_{r2} + \frac{1}{R_e}) \right. \tag{5}$$

The equations for component impedance and reactance (shown at various points of Fig. 2) can be written as:

$$Z_B = \frac{jX_m \cdot Z_\gamma}{jX_m + Z_\gamma} \tag{6}$$

$$Z_A = jX_1 + Z_\beta \tag{7}$$

$$X_1 = \omega_s L_{11} - \frac{1}{\omega_s C_{r1}} \tag{8}$$

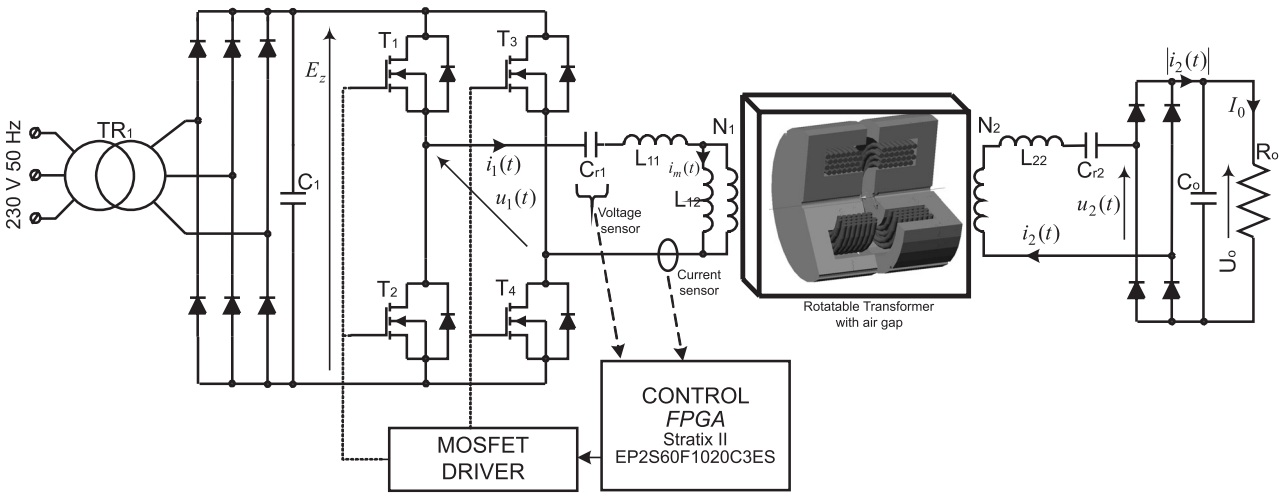

Fig. 2. Contactless energy transmission (CET) part of the power supplies system from Fig. 1.

$$X_2 = \omega_s L_{22} - \frac{1}{\omega_s C_{r2}} \tag{9}$$

$$X_m = \omega_s M \tag{10}$$

where $\omega_s = 2\pi f_s$ – operation inverter frequency.

The transfer gain of voltage CET system for SS compensation topology in Fig. 2 is:

$$G_V = \left| \frac{Z_B}{Z_A} \frac{R_e}{Z_C} \right| \tag{11}$$

From equations (3) to (11), the resulting voltage gain G_V can be expressed as:

$$G_V = \left[\left(1 + \frac{X_1}{X_m} \right)^2 + \left(\frac{X_1 + X_2 + \frac{X_1 \cdot X_2}{X_m}}{R_e} \right)^2 \right]^{-\frac{1}{2}} \tag{12}$$

It follows from equation (12) that G_V is unity at compensated frequency, even though the leakage inductances of the rotating transformer in CET system are very large. Where $\omega_0 = 2\pi f_0$ – resonance frequency (compensation frequency), is calculated for condition $X_1 = X_2 = 0$

$$\omega_o = 1/\sqrt{L_r C_r} = 1/\sqrt{L_{11} C_{r1}} = 1/\sqrt{L_{22} C_{r2}} \tag{13}$$

Based on equations (7, 8 and 13), the expressions for X_1 and X_2 can be rewritten as follows:

$$X_1 = \omega_s L_{11} \left(1 - \frac{1}{\omega^2} \right) \tag{14}$$

$$X_2 = \omega_s L_{22} \left(1 - \frac{1}{\omega^2} \right) \tag{15}$$

where: $\omega = \omega_s / \omega_0$ (16)

As result of used two halves cores and large air gap, the CET transformer operates under lower and variable magnetic coupling factor k. From equations (12) to (16) the voltage gain can be expressed as:

$$G_V = \sqrt{\left(1 + \frac{1-k}{k} \left(1 - \frac{1}{\omega^2} \right) \right)^2 + \left(Q_{ac} \left(\omega - \frac{1}{\omega} \right) \right)^2} \Bigg/ \left(1 + \frac{1-k}{2k} \left(1 - \frac{1}{\omega^2} \right) \right) \tag{17}$$

where circuit quality factor for SS compensation topology is:

$$Q_{ac} = \frac{\omega (L_{11} + L_{22})}{R_e} = \frac{\omega L_r}{R_e} \tag{18}$$

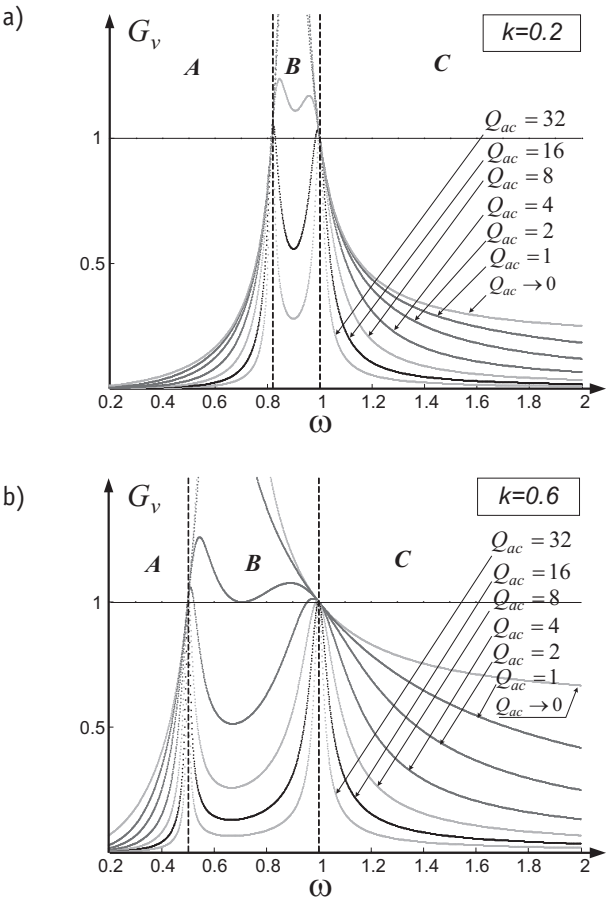

Fig. 3. The dc voltage gains of inductive CET system versus frequency for SS topology compensation. a) k = 0.2, b) k = 0.6.

The voltage gain characteristics calculated from equation (17) are shown in Fig. 3. The calculations were executed for varying frequency ω, two values coupling coefficient and various Q_{ac}. The required resonant capacitors values, for desired resonant frequency, can be expressed as follows:

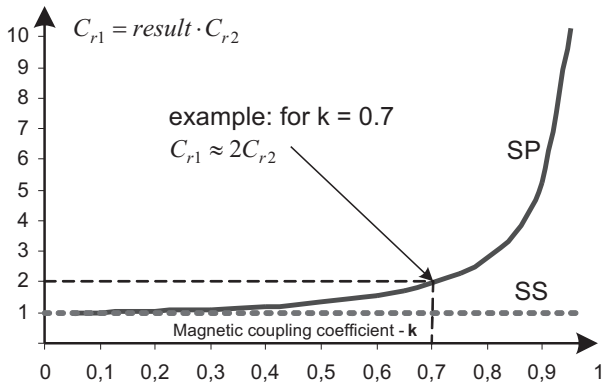

Fig. 4. Primary capacitance for SS and SP compensation versus coupling coefficient.

- for series secondary compensation

$$C_{r1} = \frac{L_{22}}{L_{11}} C_{r2} = C_{r2|L_{11}=L_{22}} \quad (19)$$

- for parallel secondary compensation

$$C_{r1} = \frac{L_{22}^2 \cdot C_{r2}}{L_{11} \cdot L_{22} - (k \cdot L_{11} \cdot L_{22})^2} = {}_{|L_{11}=L_{22}|} = \frac{1}{1-k^2} C_{r2} \quad (20)$$

The above equations are illustrated in Fig. 4.

3. FPGA Based control and protection system

The block diagram of CET control and protection system implemented in FPGA Stratix II is shown in Fig. 5. The FPGA's clock frequency is 100 MHz and the resonant switching frequency is 60 kHz. The primary capacitor voltage U_{cr1} and inverter output current i_1 are measured and sent to A/D converters via operation amplifiers. A 12-b A/D converter, AD9433 is used in the designed system. The typical analogy input signal is 5 V (V_{DD}), hence maximum of amplitude correspond to 2.5 V. The FPGA device is Stratix II EP2S60F1020C3ES.

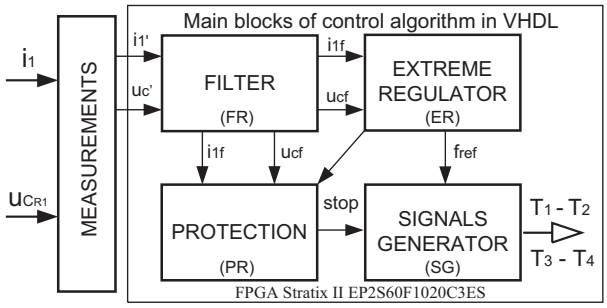

Fig. 5. Block diagram of the CET control and protection system.

To attenuate noise in input signals ($i_1^{'}$, $u_c^{'}$) from measurements block (Fig.5) a digital recursive-filtering algorithm has been applied. These filtered signals i_{1f} and u_{cf} are used in extreme regulator (ER). The ER is based on reversible counter, which determinates converter switching frequency f_{ref}. Signal f_{ref} is delivered to signal generator (SG), which generates gate pulses for MOSFET power transistors $T_1 \ldots T_4$. Also, dead time compensation is implemented in this block (SG). To guarantee stabile operations, the regulator ER in every N-period sequence searches the highest current amplitude i_{1fm} and, after comparison with previous data, adjusts reference value of switching frequency f_{ref}. Additionally, the filtered input signals i_{1f} and u_{cf} are delivered to protection block (PR), which continuously watch up and in case when limit values $i_{1f(lim)}$ and $u_{cf(lim)}$ are achieved, blocks gate pulses $T_1 \ldots T_4$. To limit current during the converter start-up, regulator (ER) sets the switching frequency higher as resonance frequency $f_{ref} > f_o$ and then in every N-period sequence reduces f_{ref} to follow the maximum of current amplitude. If the voltage and/or current amplitude reaches nominal value $i_{1f\ (N)} < i_{1f\ (lim)}$, $u_{cf\ (N)} < u_{cf\ (lim)}$, the regulator (ER) increases converter switching frequency. This results in increase of circuit impedance and as consequence current and capacitor voltage will be reduced. The period N of regulator operation has been selected experimentally $N=7$.

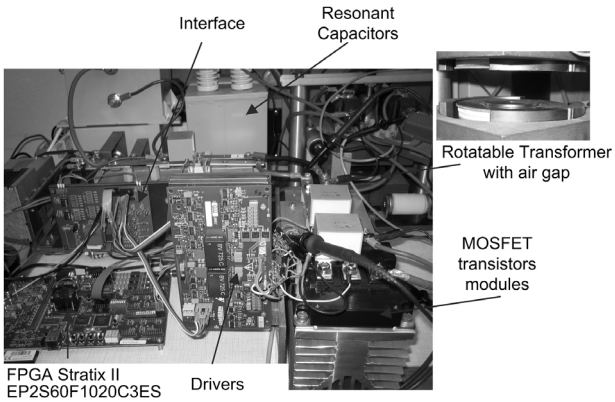

Fig. 6. Laboratory setup of 3kW contactless power supply system with rotatable transformer and series resonant MOSFET inverter.

4. Results

To verify and test performance of developed CET system, PSpice simulation model as well as 3 kW laboratory set-up has been constructed (Fig. 6). The basic parameter of rotatable transformer and resonant circuit are given in Table 1 and Fig. 8. Figures 9 to 11 show simulated and experimental oscillograms of basic waveforms in the resonant converter. Note that power MOSFET transistors operate at Zero Current Switching (ZCS) conditions. This reduces switching losses considerable and increases overall system efficiency.

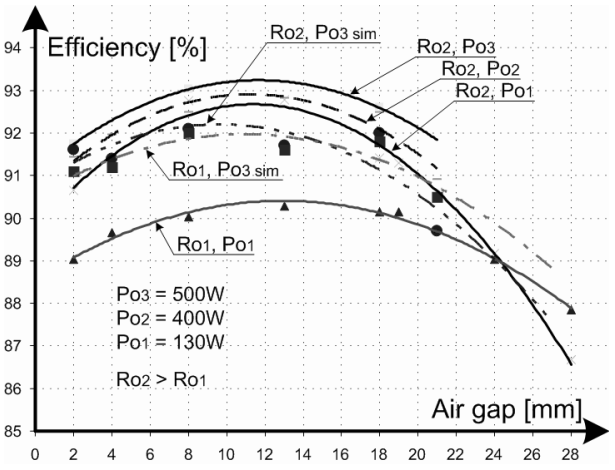

Fig. 7. Total efficiency versus air gap width and load resistance for SS compensation method, (simulated results - dashed/dotted line; experimental results -- continuous line).

Fig. 7 shows the total input-output efficiency of the CET system versus transformer air gap width and the load (for laboratory and simulation model). The efficiency curves show (Fig. 7) a slight difference between simulation and experimental values can be observed. This is result of different transistor models (in simulation we used available in PSpice library International-Rectifier transistors

model (IRGPC50S), whereas in the laboratory prototype Semikron MOSFET power transistors (SKM120B020) have been mounted). Note that for higher load resistances higher efficiency can be achieved, but the circuit becomes more sensitive for magnetic coupling coefficient changes.

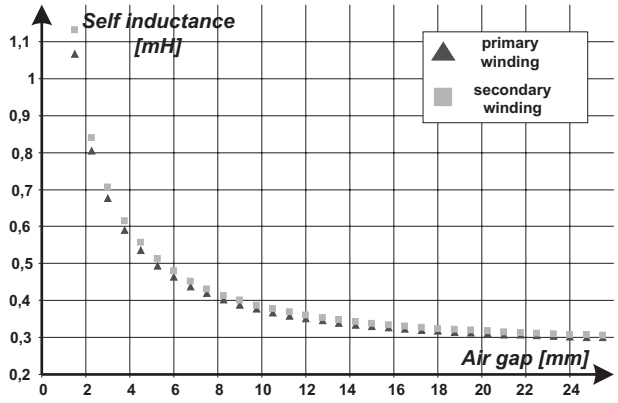

Fig.8. Measured self-inductance primary and secondary winding of rotatable transformer in laboratory model.

Simulation Experimental

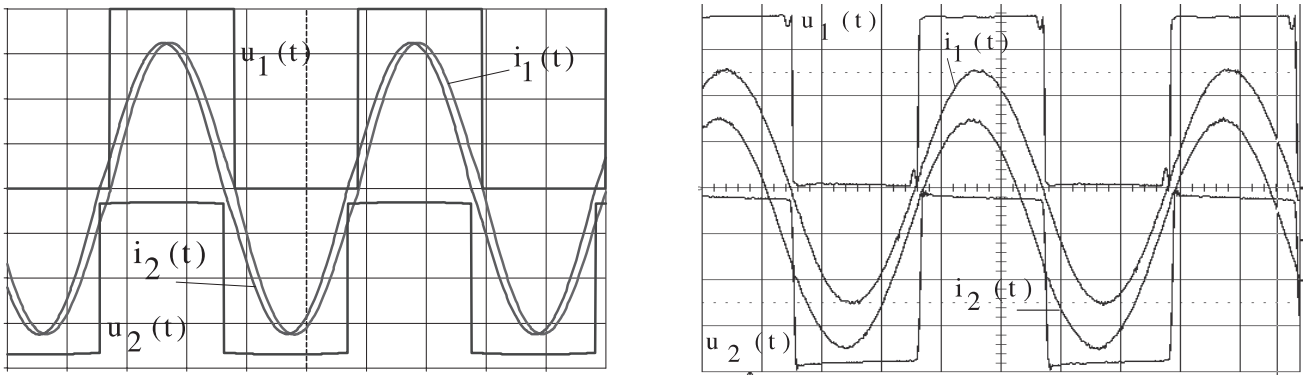

Fig. 9. Steady-state waveforms of the voltages u_1, u_2, and currents i_1, i_2. Converter operation with resonance frequency (5s/div, 50V/div, 4A/div).

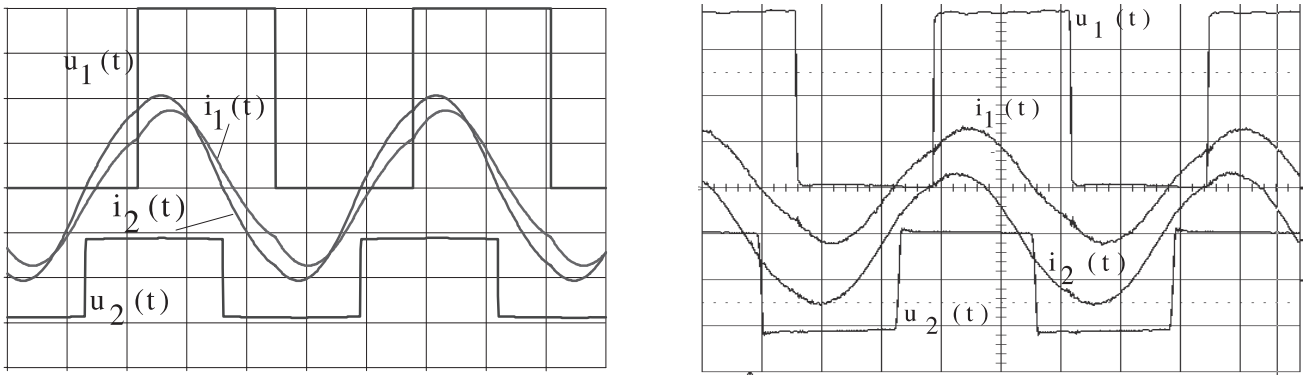

Fig. 10. Steady-state waveforms of the voltages u_1, u_2,, and currents i_1, i_2. Converter operation below resonance frequency (5s/div, 50V/div, 4A/div).

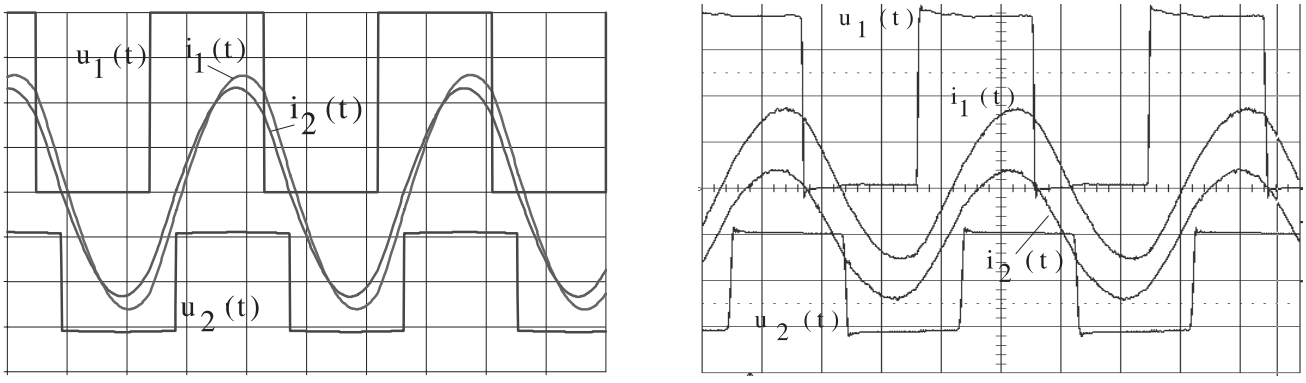

Fig. 11. Steady-state waveforms of the voltages u_1, u_2,, and currents i_1, i_2. Converter operation above resonance frequency (5s/div, 50V/div, 4A/div).

Table 1. Parameters of rotating transformer and resonant circuit.

Parameter	Value	Unit
N_1	32	coils
N_2	32	coils
L_{11}	166.5	H
L_{12}	203.5	H
L_{22}	166.5	H
M	203.5	H
k	0.55	-
C_{R1}	63	nF
C_{R2}	63	nF
C_1	1000	F
C_0	100	F
R_0	16	ohm
Adjustable air gap	10.5	mm

5. Summary and conclusion

This paper presents a novel Contactless Power Supply (CPS) system for robot and manipulators. The core of the system is inductive Contactless Energy Transmission (CET) with rotatable transformer and series resonant inverter operating at 60 kHz switching frequency. The control and the protection system have been implemented in FPGA Stratix II EP2S60F family. To compensate high leakage inductance of the rotatable transformer with large air gap and converter switching losses, the series resonant capacitive circuit has been used. Extreme regulator, which follows the instantaneous value of primary peak current, adjusts the resonance frequency and guaranties zero current switching (ZCS) conditions for power MOSFET transistors of the inverter.

Theoretically, there is no power transfer limit, even with low coupling coefficient, if the circuit operates with the resonance frequency of secondary current, in compensated primary winding conditions, and resonant frequency of primary current is equal to secondary. From (19) it can be concluded that in SS compensation topology both resonant capacitances are equal, if $L_{11} = L_{22}$. The design procedure has been verified by simulation and experimental results measured on the 3 *kW* laboratory set-up. The total efficiency achieves 0,93–0,85 for rotatable transformer air gap 0.1 up to 2.8 cm, respectively.

AUTHORS

Artur Moradewicz* - Electrotechnical Institute IEl, ul. M. Pożaryskiego 28; 04-703 Warsaw, Poland; e-mail: a.moradewicz@iel.waw.pl.

Marian P. Kaźmierkowski - Director of the Institute of Control and Industrial Electronics, Faculty of Electrical Engineering, Warsaw University of Technology, ul. Koszykowa 75, 00-662 Warsaw, Poland.

* Corresponding author

References

[1] W. Erickson: *Fundamentals of Power Electronics*, Kluwer Academic Publisher, 1999.

[2] M. P. Kazmierkowski and J. T. Matysik, *Introduction into signal and power electronics*, Warsaw, Warsaw University of Technology Publisher, 2005 (in Polish).

[3] A. Moradewicz, "*Study of Wireless Energy Transmission Systems Using Inductive Coupling*". In: *Proc. of International Conf. PELINCEC*, 2005, Warsaw, Poland (CD).

[4] J. T. Matysik: "*A New Method of Integration Control with Instantaneous Current Monitoring for Class D*, *IEEE Trans. on Industrial Electronics*, vol. 53, no. 5, 2006, pp. 1561-1576.

[5] J. Hirai, T. W. Kim, and A. Kawamura, "Study on intelligent battery charging using inductive transmission of power and information", *IEEE Trans. on Power Electronics,* vol. 15, no. 2, 2000, pp. 335-344.

[6] Ch. Apneseth, D. Dzung, S. Kjesbu, G. Scheible, and W. Zimmermann, "Introduction wireless proximity switches", ABB Review, no. 4, 2002, pp. 42-49.

[7] A. Esser and H.-Ch. Skudelny, "A New Approach to Power Supplies for Robots", *IEEE Trans. on Industry Applications*, vol. 27, no. 5, 1991, pp. 872-875.

[8] K. O'Brien, G. Scheible, H. Gueldner, "Analysis of Wireless Power Supplies for Industrial Automation Systems". In: *Proc. of IEEE-IECON'03*, Roanoke, Virginia, USA, 2nd-6th Nov. 2003, vol. 1, pp. 367 - 372.

[9] J. Lastowiecki and P. Staszewski, "Sliding Transformer with Long Magnetic Circuit for Contactless Electrical Energy Delivery to Mobile Receivers", *IEEE Trans. on Industrial Electronics*, vol. 53, no. 6, 2006, pp. 1943-1948.